Low-Sidelobe Cavity-Backed Slot Antenna Array With Simplified Feeding Structure for Vehicular Communications

Rui-Sen Chen, *Student Member, IEEE*, Lei Zhu, *Fellow, IEEE*, Sai-Wai Wong, *Senior Member, IEEE*, Xu-Zhou Yu, Yin Li, *Member, IEEE*, Long Zhang, *Member, IEEE*, and Yejun He, *Senior Member, IEEE*

***Abstract*—In this article, low-sidelobe cavity-backed slot antenna array with simplified feeding structure for vehicular communication is proposed. Conventional low-sidelobe antennas were realized using power dividing network to obtain the in-phase and nonuniform-amplitude excitation, which causes complicated antenna's structure and design. To tackle these challenges, a simplified feeding method without using power dividing network is introduced to design the low-sidelobe slot antenna array. The slots at the top walls serve as the radiation elements, and the slots are directly fed by the electric field of the cavity mode. Nonuniform amplitude is obtained by simply modifying the slots' sizes and positions, while the in-phase excitation of the elements is remained. The nonuse of power dividers brings out a simpler antenna structure than conventional full-metal waveguide-based antennas. Besides, the full-metal structure introduces a high power-handling capacity. Then, two linear arrays with 1 × 4, 1 × 7 elements and a planar array with 5×4 elements are presented to show the design feasibility. Finally, the 5 × 4 antenna array is fabricated and measured, which can achieve 18.2 dBi gain, −20 dB sidelobe level, 94% radiation efficiency, and -42 dB cross-polarization. Good agreement between measurement and simulation verifies the feasibility of the proposed design concept.**

***Index Terms*—Low-sidelobe, cavity-backed slot antenna array, vehicular communication, simplified feeding structure, full-metal.**

Manuscript received October 8, 2020; revised January 22, 2021; accepted March 7, 2021. Date of publication March 23, 2021; date of current version May 5, 2021. This work was supported in part by the National Natural Science Foundation of China under Grants 62071306, 61801299, and 61871433, in part by the Natural Science Foundation of Guangdong Province under Grant 2018A030313481, in part by the Shenzhen Science and Technology Program under Grants JCYJ20200109113601723, GJHZ20180418190529516, JSGG20180507183215520, JCYJ20180305124543176, and JCYJ20190728151457763, and in part by the Shenzhen University Research Startup Project of New Staff under Grant 860-000002110311. The review of this article was coordinated by Prof. Yue Gao. (*Corresponding authors: Sai-Wai Wong; Yejun He.*)

Rui-Sen Chen is with the College of Electronics and Information Engineering, Shenzhen University, Shenzhen 518060, China, and also with the Department of Electrical and Computer Engineering, Faculty of Science and Technology, University of Macau, Macau SAR, 999078, China (e-mail: crs13763378709@163.com).

Lei Zhu is with the Department of Electrical and Computer Engineering, Faculty of Science and Technology,University of Macau, Macau SAR 999078, China (e-mail: leizhu@umac.mo).

Sai-Wai Wong, Xu-Zhou Yu, Yin Li, Long Zhang, and Yejun He are with the College of Electronics and Information Engineering, Shenzhen University, Shenzhen 518060, China (e-mail: wongsaiwai@ieee.org; 1844723487@qq.com; liyinuestc@gmail.com; long.zhang@szu.edu.cn; heyejun@126.com).

Digital Object Identifier 10.1109/TVT.2021.3067894

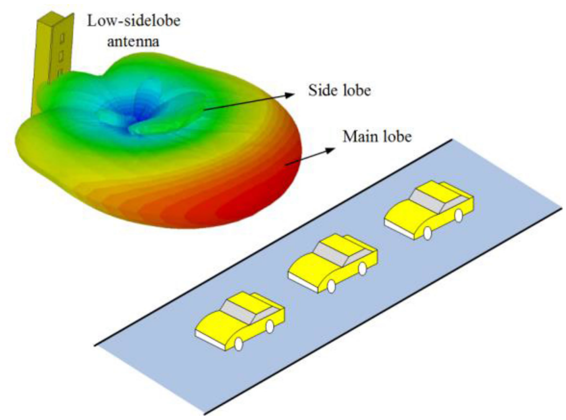

Fig. 1. Application of low-sidelobe antenna for vehicular communication.

I. Introduction

Antenna is a critical component in wireless communication systems, such as vehicular communication and mobile communication, as it acts an important role in transmitting and receiving target's signal of the electronic devices. Antennas designed by PCB process [1]–[7] have small size and low cost. Although the antennas implemented by full-metal structure [8]–[13] have large size and high cost, they have the advantages of high gain, high efficiency, and high power handling capacity, which are highly demanded in long-distance and high-power communication systems.

Low-sidelobe antenna can reduce the interference produced by the side lobe, such as the noise signal outside the road can be effectively reduced due to the low gain of the side lobe, as shown in Fig. 1, and then improve the resolution capability of the main lobe. Thus, low sidelobe is a good property for vehicular communication systems to improve the communication quality between vehicles and infrastructures. Low-sidelobe antenna can be implemented by different structures, such as microstrip [14]–[17], substrate integrated waveguide (SIW) [18], [19] and metal cavities [20]–[22]. Nonuniform amplitude distribution is a popular and effective way to design the low-sidelobe antenna arrays [14]–[22]. The pattern synthesis includes binomial distribution [14], Chebyshev distribution [15], [16], [21], and Taylor distribution [20], [22]. The nonuniform amplitudes of the antenna elements of these antennas were obtained by using unequal-power dividing network. In [14], a 4×4 low-sidelobe microstrip antenna array is proposed, the nonuniform amplitude is obtained using unequal-power dividers, and −17 dB sidelobe level was achieved. In [20], a modified T-junction power divider with equal phase and unequal power is introduced to feed the elements and then obtain a nonuniform amplitude distribution, this 16×16 array can achieve −25 dB sidelobe level. However, the aforementioned low-sidelobe antennas suffer from a complicated structure due to the utilization of power dividers, especially for full-metal slot antennas. In [23], a low-sidelobe travelling slot antenna was reported. The feed of the elements did not require the power dividers. However, the phase shifters were required to obtain the in-phase excitation. Thus, the conventional low-sidelobe antenna arrays usually have complicated feeding structure to obtain desired amplitude distribution and in-phase excitation.

Up to now, there are two main wireless communication standards for V2X (vehicle to everything) communications, one is the dedicated short-range communications (DSRC) and the other is the cellular V2X (C-V2X) [24], [25]. DSRC with frequency band of 5.85–5.925 GHz aims at supporting direct communication between the vehicles and roadside unit. The C-V2X enables vehicles to communicate with everything through base stations in licensed band for telecommunication operators [24], [25]. Today, the 5th-generation (5G) communication and technology is emerging, and the commercial application of the 5G communication at sub-6G band (such as 3.3G HZ∼3.8 GHz) is starting. The C-V2X communication will also cater to this newly-emerging wireless system, which can help C-V2X to enhance the road safety and improve the connectivity among vehicles or between the vehicles and other things. The current standard is commonly referred as LTE-V (long-term evolution-vehicle) [26].

In this paper, novel low-sidelobe full-metal slot antenna arrays with simplified feeding structure for 5G-V2X communication are proposed. Taking advantage of all the slots directly excited by TE_{101} cavity mode, a simplified feeding network for the antenna array is proposed without using power dividers. The nonuniform-amplitude distribution is obtained by simply adjusting the sizes and positions of the radiation slots. While the in-phase excitation of the elements is almost remained. Three design examples are presented to show the design feasibility. The proposed slot arrays demonstrate the merits of high radiation efficiency, high gain, low-sidelobe level, low design complexity, and high power-handling capacity. Finally, the 5×4 elements array is fabricated and measured to verify the design concept.

II. Basic Design Principal

A. *Simplified Feeding Structure Based on Cavity Mode*

To show the operating mechanism of proposed feeding technique, we firstly introduce an antenna array with four radiation slots, as shown in Fig. 2. This antenna array is composed of a resonant cavity with one feeding slot at bottom wall and four slots at top wall, and a coaxial-to-waveguide transition formed by a feeding cavity and a probe. Here, the coaxial-to-waveguide transition serves as a waveguide input. The four slots are initially

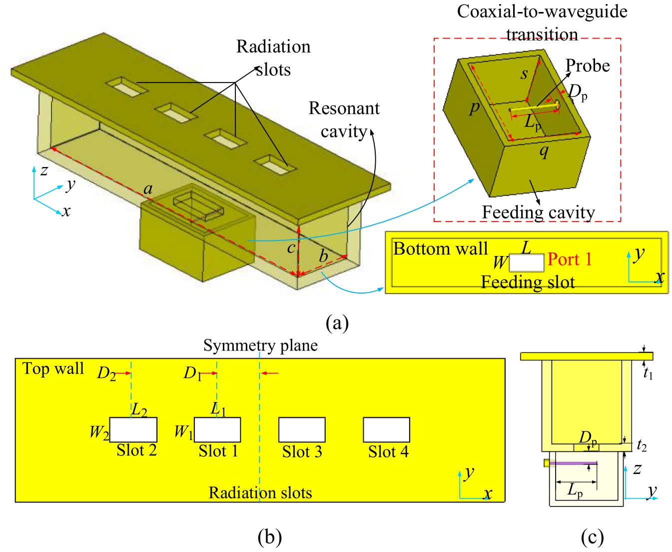

Fig. 2. Configuration of the four-element antenna array using TE_{101} cavity mode: (a) Perspective view; (b) Top view; (c) Side view.

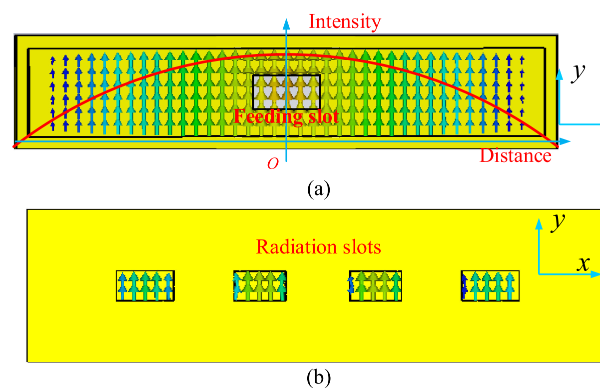

Fig. 3. (a) Electric field distribution inside the resonant cavity; (b) Electric field distribution on the multiple radiation slots.

set identical and are symmetrically arranged on the top wall. The relevant parameters are marked in the Fig. 2.

The TE_{101} mode of the rectangular waveguide cavity can be excited by a feeding slot perpendicular to the direction of electric field (*E*-field), as shown in Fig. 3(a). The resonant frequency of TE_{101} mode can be obtained using (1), where v represents the speed of light in free space.

$$f_{TE_{101}} = \frac{v}{2}\sqrt{\left(\frac{1}{a}\right)^2 + \left(\frac{1}{c}\right)^2} \quad (1)$$

It can be seen that the *E*-field distribution is symmetrical about the origin, and the intensity in the center part is larger than the side part. The *E*-field in the slots is shown in Fig. 3(b), all the slots are fed by the *E*-field of TE_{101} mode and correspond to the radiation. These slots are fed without using any power dividers, which can reduce the complexity and over-all size of the antenna array. Besides, the amplitude and phase excitation of the slots are symmetrical.

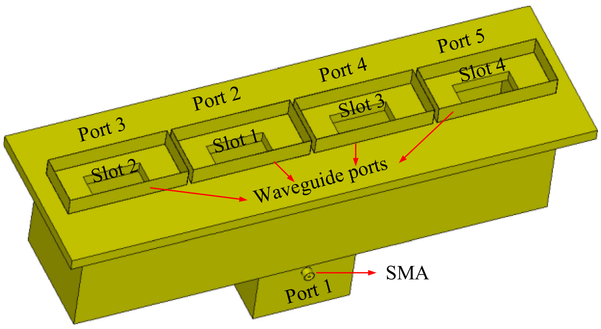

Fig. 4. Extraction model for the amplitude and phase.

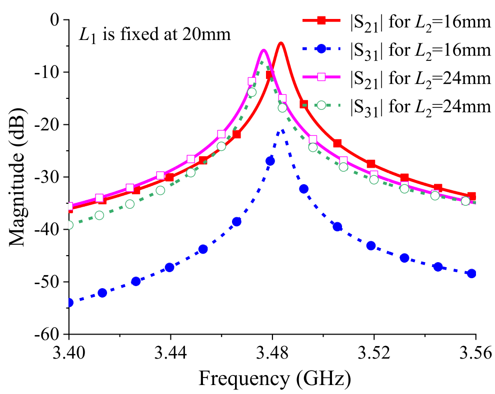

(a)

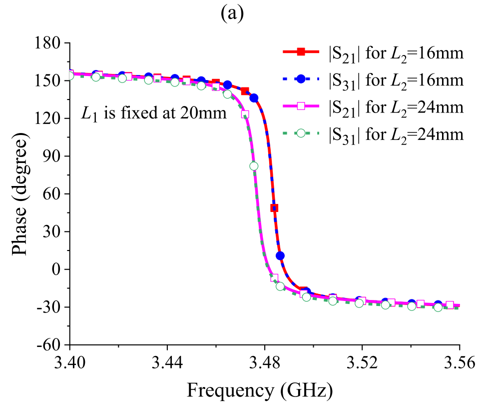

(b)

Fig. 5. Simulated $|S_{21}|$ and $|S_{31}|$ versus varying L_2: (a) Magnitude; (b) Phase.

B. Analysis of Amplitude Ratio and Phase Difference

For conventional low-sidelobe antenna array, the nonuniform amplitude distribution is obtained by controlling the internal coupling strengths of the multistage and multipath power dividing network. While for the proposed design method, the nonuniform amplitude distribution is obtained by simply adjusting the sizes and positions of the radiation slots.

Fig. 4 shows the simulation model for extracting the magnitude and phase of elements, and the simulated results are shown in Fig. 5(a) and (b). The port information is provided in Fig. 4. As the exaction amplitude and phase is symmetry along *x*-axis, only the parameters of $|S_{21}|$ and $|S_{31}|$ are discussed. It can be seen that the increasing length of slot 2 enlarges the magnitude of $|S_{31}|$ (Related to slot 2), as the increasing size of the slot

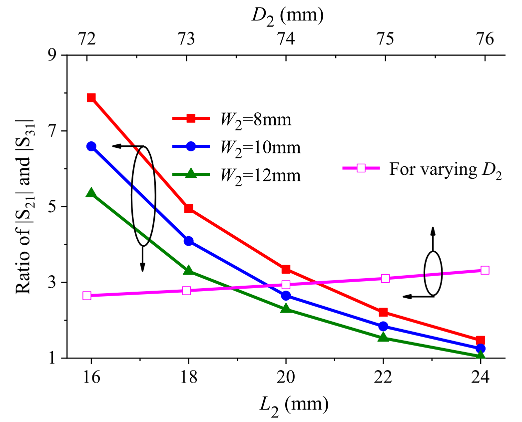

(a)

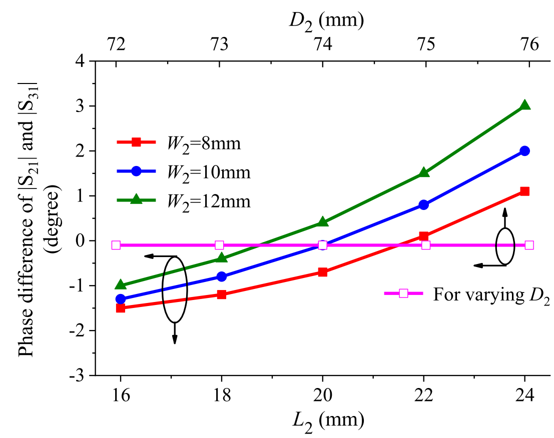

(b)

Fig. 6. Excited results of $|S_{21}|$ and $|S_{31}|$ against L_2, W_2, and D_2: (a) Amplitude ratio; (b) Phase difference.

can enhance the radiation energy of the TE_{101} mode, which consequently decrease the amplitude ratio of $|S_{21}|/|S_{31}|$. Fig. 5(b) indicates that the varying length of slots has very little effect on the phase difference between slot 1 and slot 2. The same phase of the slots is achieved due to the fact that the EM field of TE_{101} propagates along *z*-direction, and the slots are located in a same-distance wave front along the propagation direction. The in-phase excitation is required for designing the low-sidelobe arrays using nonuniform amplitude distribution.

Fig. 5 gives the direct insight into the achievement of the nonuniform amplitude and equal phase of proposed antenna array by modifying the size of the slots. For the practical design of the low-sidelobe antenna, it is the amplitude ratio between the elements that corresponds to the achievement of a low sidelobe, and different sidelobe levels require different amplitude ratios. Therefore, the adjustment of amplitude ratio is then discussed.

Fig. 6(a) shows the amplitude ratio of slot 1 and slot 2 ($|S_{21}|/|S_{31}|$) against L_2, W_2, and D_2, which are the parameters belonging to slot 2. The data indicates that the increasing length or width of the slots leads to a decreasing amplitude ratio. A larger distance of the slot 2, i.e., D_2, results in smaller excited amplitude of slot 2 and then enlarges the ratio. Therein, the length and width of the slot have greater effect than the distance between the slot and the origin. Fig. 6(b) indicates that the phase

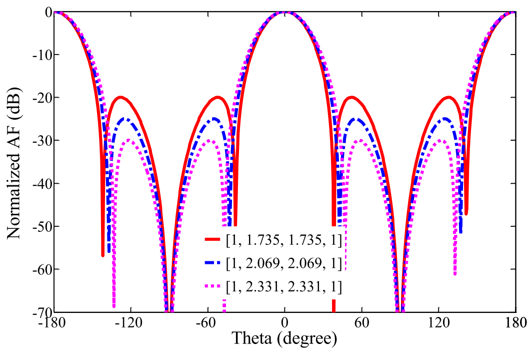

Fig. 7. Calculated results of the four-element Chebyshev array with different amplitude vectors.

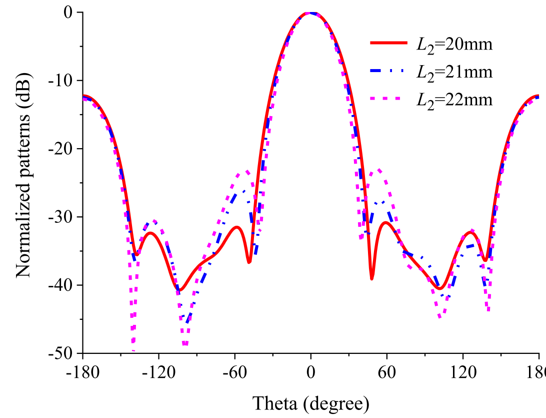

Fig. 8. Simulated radiation patterns at XZ-plane of four-element array versus varying L_2. The varying L_2 produces a varying amplitude ratio, as shown in Fig. 5(a), which consequently produces a varying sidelobe level.

difference between slot 1 and slot 2 is less than 3 degree in such large tuning range of the amplitude ratio (from 1:1 to 8:1).

Similarly, the parameters belonging to slot 1, i.e., L_1, W_1, and D_1, can be also used to modify the amplitude ratio.

In a word, compared to the conventional design method of low-sidelobe antenna arrays, the proposed one shows the following merits:

1) No power divider is utilized to feed the elements, which brings out a simple antenna structure and easy fabrication.
2) Nonuniform amplitude distribution can be easily obtained by simply modifying the slots' dimensions.
3) The equal phase of the all the slots are self-remained during the adjustment of the amplitude ratio without using additional feeding structures.

III. Design of Low-Sidelobe Slot Antenna Array

A. Four-Element Low-Sidelobe Slot Array

According to the Chebyshev array presented in [27], [28], the array factor (AF) and the amplitude vector of the arrays with $2n$ and $2n+1$ elements are given as follow:

$$AF_{2n}(dB) = 20\lg\left|2\sum_{i=1}^{n} a_i \cos(\frac{2i-1}{2}kd\sin\theta)\right| \quad (2)$$

$$AF_{2n+1}(dB) = 20\lg\left|2\sum_{i=1}^{n+1} a_i \cos[(i-1)kd\sin\theta]\right| \quad (3)$$

$$V_{2n} = \left[\alpha_n \cdots \alpha_2\ \alpha_1 \quad \alpha_1\ \alpha_2 \cdots \alpha_n\right] \quad (4)$$

$$V_{2n+1} = \left[\alpha_{n+1} \cdots \alpha_2\ \alpha_1\ \alpha_2 \cdots \alpha_{n+1}\right] \quad (5)$$

where a_n represents the amplitude of the element, k is the propagation constant, d is the distance between the elements.

The sidelobe level of the array factor of four-element array calculated using (2) is depended on the amplitude ratio a_1/a_2, which is equivalent to the ratio of $|S_{21}|/|S_{31}|$ shown in Fig. 6(a). According to [28], the amplitude vectors of the four-element array with -20dB/-25dB/-30dB sidelobe levels are given in (6), where the amplitude a_2 is normalized as 1. The calculated results are plotted in Fig. 7. It can be seen that a lower sidelobe level requires a larger amplitude ratio.

$$V_4^{20\,\mathrm{dB}} = [1 \quad 1.735 \quad 1.735 \quad 1]$$

$$V_4^{25\,\mathrm{dB}} = [1 \quad 2.069 \quad 2.069 \quad 1]$$

$$V_4^{30\,\mathrm{dB}} = [1 \quad 2.331 \quad 2.331 \quad 1] \quad (6)$$

In the practical design of proposed slot array, the different amplitude ratio is obtained by modifying the slots' sizes and the distance between the slots and the origin, as discussed in Fig. 6(a). Besides, Fig. 7 shows that a different ratio of a_1/a_2 produces a different sidelobe level. Thus, by modifying the slots' size, a different sidelobe level will be obtained. Fig. 8 shows the simulated radiation pattern with the function of varying L_2. It can be seen that a larger L_2 produces a higher sidelobe level, as a larger L_2 causes a lower amplitude ratio, which is shown in Fig. 6(a).

Thus, the proposed design concept features a simple feeding structure and an easy achievement of designing low-sidelobe antenna arrays. Here, two arrays with -20 dB and -30 dB sidelobe level, called Type-I and Type-II, are investigated to show the feasibility of designing antennas with different sidelobe levels. The amplitude vectors of Type I and Type II are [1, 1.735, 1.735, 1] and [1, 2.331, 2.331, 1], respectively.

Then, these values are modified to match the given ratios using the previous extracted method shown in Fig. 6. The final $|S_{11}|$ and realized gain is shown in Fig. 9(a), and the normalized radiation pattern is shown in Fig. 9(b). Both of them have a good impedance matching at the operation frequencies. For the prescribed -20 dB sidelobe level, the simulated sidelobe is about -22 dB with an 11.7 dBi gain, while for the prescribed -30 dB suppression level, simulated sidelobe is about -30 dB with an 11.3 dBi gain. Thus, a trade-off should be made between the suppression level and radiation gain, which also indicates that this proposed method has flexibility in designing antenna arrays with varied sidelobe level. The final dimensions of them are provided in Table I.

B. Seven-Element Low-Sidelobe Slot Array

The conventional low-sidelobe antenna arrays based on the unequal-power dividing network were usually limited in designing even number of elements. While the proposed design

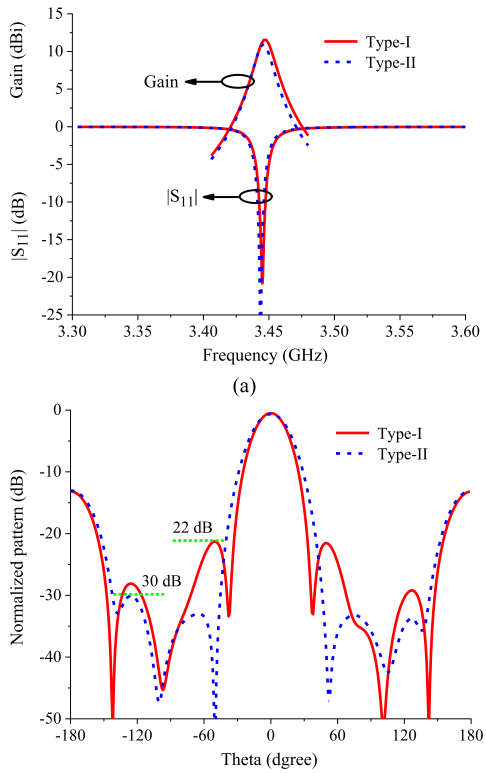

Fig. 9. Simulated results of two type of four-element low-sidelobe antenna array: (a) $|S_{11}|$ and realized gain; (b) Normalized pattern at XZ-plane.

TABLE I
DIMENSIONS OF TWO FOUR-ELEMENT ANTENNAS (UNIT: mm)

Common	a	b	c	p	q	s	t_1	t_2	D_1	D_2
	190	36	43.4	48	30	28	2	3	21	64
Type-I	L	L_1	L_2	W	W_1	W_2	L_P	D_P		
	25	20	22.6	10	10.6	10	28	5.6		
Type-II	L	L_1	L_2	W	W_1	W_2	L_P	D_P		
	24.5	21.6	20.8	10	10.5	10	26	7		

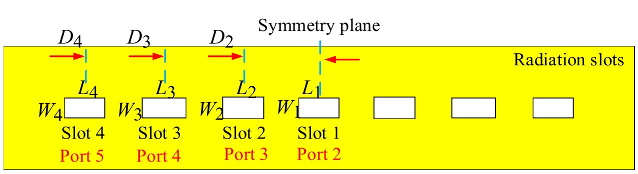

Fig. 10. Top view of the seven-element low-sidelobe antenna array (Other structures are identical to the four-element array in Fig. 2, including the definition and position of port 1).

method can be applied to array with odd number of elements. Here, a seven-element slot array is presented, and the top view with marked dimensions is shown in Fig. 10. The other structures and marked dimensions are identical to the four-element array shown in Fig. 2. Similarly, the adjustments of the amplitude ratio and phase difference between the slots are firstly discussed.

Fig. 11 shows the simulated amplitudes and phases of the slots of the seven-element array. If the sizes of the slots are identical, all the slots are in-phase fed, but with different amplitude excitation, and the amplitude vector is [1, 2.89, 4.87, 6.4, 4.87, 2.89, 1], as shown in Fig. 9(a). When the slots are set with

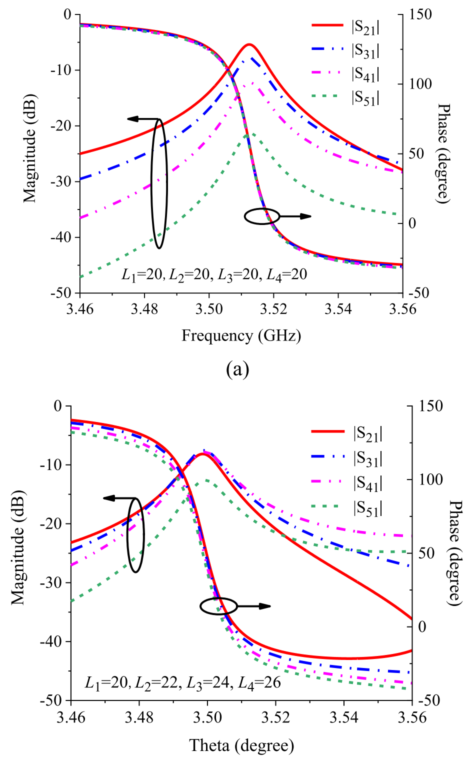

Fig. 11. Simulated amplitudes and phase of seven-element array with different slots' lengths: (a) $L_1 = 20$, $L_2 = 20$, $L_3 = 20$, $L_4 = 20$; (b) $L_1 = 20$, $L_2 = 22$, $L_3 = 24$, $L_4 = 26$.

different lengths, e.g., $L_1 = 20$, $L_2 = 22$, $L_3 = 24$, $L_4 = 26$ (All in mm), the slots have different phase excitation, but the difference are within 10 degrees. Besides, the amplitude vector is [1, 1.75, 1.8, 1.68, 1.8, 1.75, 1]. It can be concluded that the phase differences between the slots are very small under a large variation of the amplitude ratio. Thus, a low-sidelobe antenna can be achieved by properly modifying the sizes of the slots. Similarly, to show the feasibility of design antenna array with different sidelobe levels, two seven-element arrays with -20dB and -30 dB sidelobe level are presented, and called Type-III and Type-IV antennas, respectively. The amplitude vectors of them are [1, 1.28, 1.68, 0.92, 1.68, 1.28, 1] and [1, 2.15, 3.31, 1.89, 3.31, 2.15, 1], respectively.

Then, the amplitudes of the slots are modified to match the given ratios using the previous extracted method shown in Fig. 6. The final $|S_{11}|$ and realized gain is shown in Fig. 12(a), both of them has a good impedance matching at the operating frequencies. The normalized radiation pattern is shown in Fig. 12(b). For the prescribed -20 dB sidelobe level, the simulated sidelobe is about -22 dB with a 13.3 dBi gain, while for the prescribed -30 dB suppression level, simulated sidelobe is about -32 dB with a 12.7 dBi gain. The final dimensions of them are provided in Table II.

C. Design of Low-Sidelobe Planar Slot Array

The proposed design method can be used to design low-sidelobe planar slot array. The linear array can only achieve

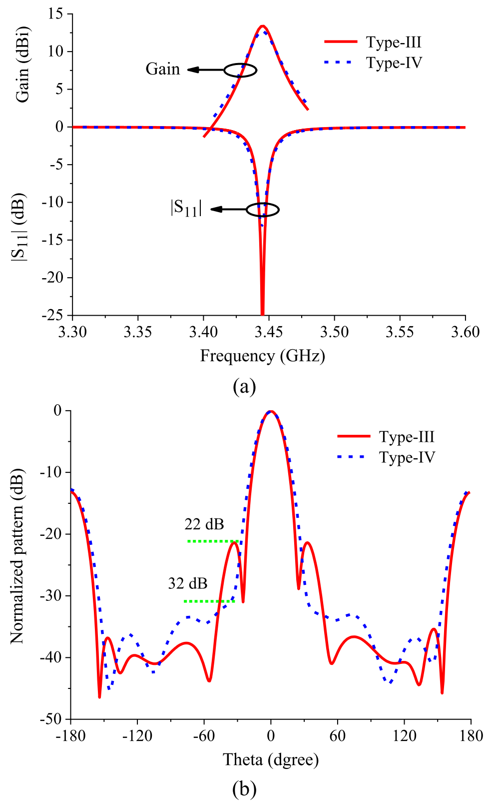

Fig. 12. Simulated results of two type of seven-element low-sidelobe antenna arrays: (a) $|S_{11}|$ and realized gain; (b) Normalized pattern at XZ-plane.

TABLE II
DIMENSIONS OF TWO SEVEN-ELEMENT ANTENNAS (UNIT: mm)

Common	a	b	c	p	q	s	t_1	t_2	D_2	D_3	D_4	L_p	D_p
	310	36	42.4	38	30	28	3	3	41	84	127	26	7
Type-III	L	L_1	L_2	L_3	L_4	W	W_1	W_2	W_3	W_4			
	26.6	22	22	24	22	14	11	12	11	11			
Type-IV	L	L_1	L_2	L_3	L_4	W	W_1	W_2	W_3	W_4			
	28	22	21	23	21	14.4	11	12	10	11			

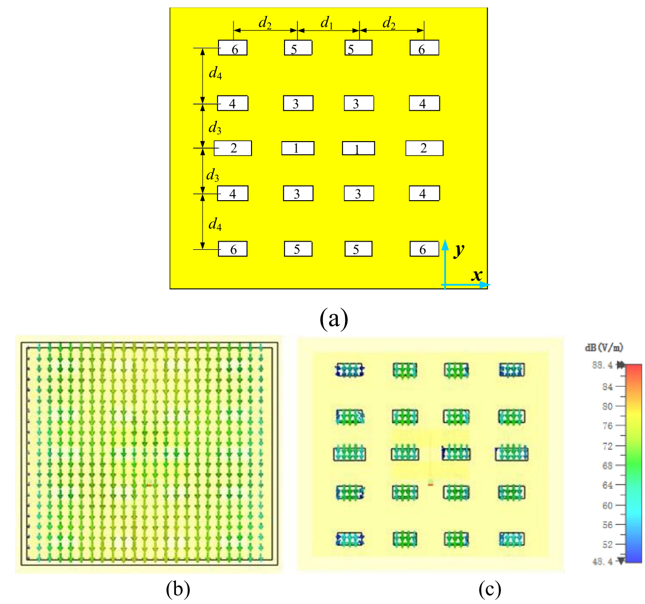

Fig. 13. Proposed 5×4-element antenna array: (a) Top view; (c) Electric field inside the cavity; (c) Electric field in the radiation slots.

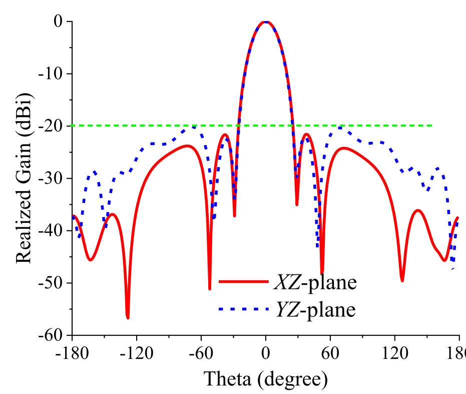

Fig. 14. Simulated radiation pattern at 3.44 GHz. Dimensions (Unit: mm): $a = 230$, $b = 200$, $c = 44$, $p = 75$, $q = 48$, $s = 31$, $d_1 = 50$, $d_2 = 54$, $d_3 = 37$, $d_4 = 46$, $D_{\mathrm{p}} = 12$, $L = 66.2$, $L_1 = 26.5$, $L_2 = 31$, $L_3 = 24.5$, $L_4 = 25$, $L_5 = 22.5$, $L_6 = 23.5$, $L_{\mathrm{P}} = 42$, $W = 13$, $W_1 = 10.9$, $W_2 = 11.9$, $W_3 = 12$, $W_4 = 12$, $W_5 = 12$, $W_6 = 12$, $t_1 = 4$, $t_2 = 3$, $t_3 = 5$, $h = 11$.

low sidelobe in one observed plane, which can be seen from Fig. 1. In order to achieve low sidelobe level in both *XZ*-plane and *YZ*-plane, a 5×4-element antenna array is proposed, and the configuration is plotted in Fig. 13(a). The realization of planar array can also help to enhance the radiation gain. This antenna has four-column and five-row elements in *x*- and *y*-axis, respectively. The slots are arranged symmetrically along *x* and *y* axis, and have symmetrical excitation of phase and amplitude about the origin.

Thus, the same marked number of slots shown in Fig. 13(a) have the same amplitude and phase and excitation. The sizes of the slots are L_i and W_i, where $i = 1, 2, 3, 4, 5, 6$, which are the marked labels shown in Fig. 13(a). The electric field inside the resonant cavity and on the radiation slots are shown in Fig. 13(b) and (c). It can be seen that the antenna operates at TE_{101} mode, and all the slots have electric field with a same direction, of the electric field of TE_{101} mode. Thus, all the slots are directly fed by the cavity mode TE_{101}.

The target is to achieve 20 dB sidelobe suppressions in both *XZ*-plane and *YZ*-plane. The amplitude vectors of the four-element in *x*-axis and five-element in *y*-axis are [1, 1.736,1.736, 1] and [1.035, 1.664, 1, 1.664, 1.035], respectively. Thus, the amplitude vector of 5×4 array is given in (5), where the four elements in each row (*x*-axis) should be matched to the amplitude vector [1, 1.736, 1.736, 1] and five elements in each column (*y*-axis) should be matched to the amplitude vector [1.035, 1.664, 1, 1.664, 1.035]. The desired amplitude ratio can be obtained by properly adjusting the slots' size. After the adjustment and optimization, a 5×4 planar antenna array with simulated sidelobe level of −23 dB at *XZ*-plane and −20 dB at *YZ*-plane is achieved. The maximum realized gain is 18.3 dBi, as shown in Fig. 14.

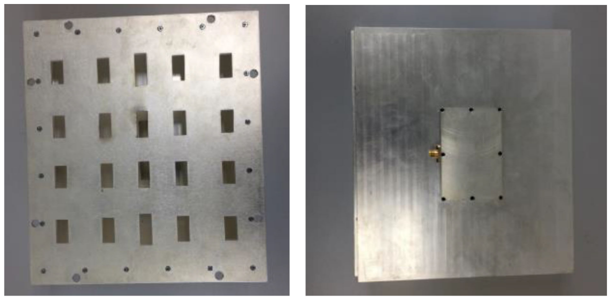

Fig. 15. Photographs of the proposed 5×4 antenna array : (a) Top view and (b) Bottom view.

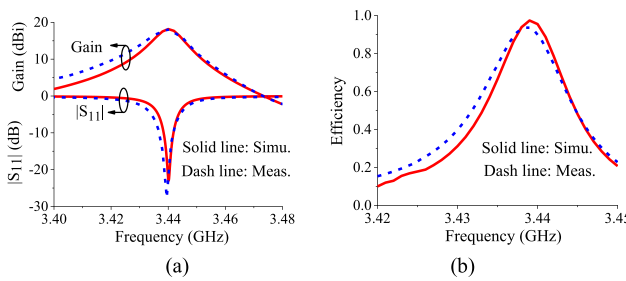

Fig. 16. Simulated and measured results of the proposed 5×4 antenna array : (a) Return loss and realized gain and (b) Radiation efficiency.

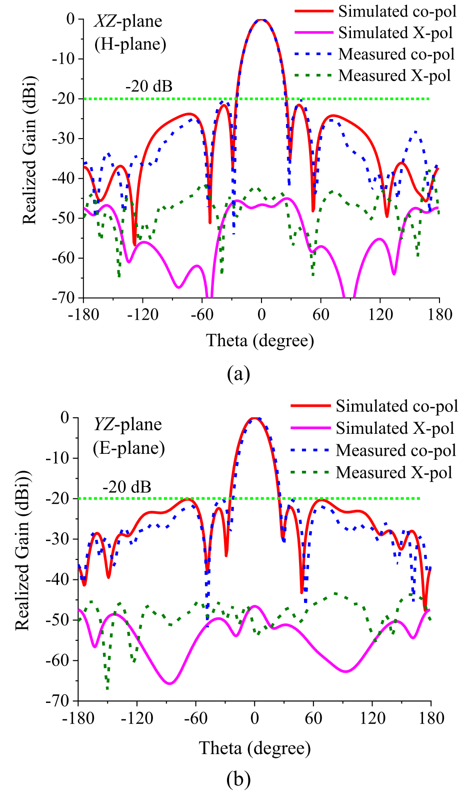

Fig. 17. Simulated and measured patterns at 3.44GHz: (a) *XZ*-plane and (b) *YZ*-plane.

The simulated radiation efficiency is 97.4%.

$$V_{5\times4}^{20dB} = \begin{bmatrix} 1.035 & 1.8 & 1.8 & 1.035 \\ 1.664 & 2.89 & 2.89 & 1.664 \\ 1 & 1.736 & 1.736 & 1 \\ 1.664 & 2.89 & 2.89 & 1.664 \\ 1.035 & 1.8 & 1.8 & 1.035 \end{bmatrix} \quad (7)$$

IV. Experimental Results

For proof-of-concept, the proposed 5×4 antenna array is fabricated using silver-plated lossy copper and based on the computer numerical control (CNC) process. The photograph of the proposed antenna is provided in Figs. 15(a) and (b). The comparison between simulated and measured results is plotted in Figs. 16 and 17. The measured return loss is 25 dB at 3.44 GHz, the maximum gain and radiation efficiency are 18.2 dBi and 94%, respectively. As shown in Figs. 17(a) and (b), the sidelobe levels are better than −20 dB at both XZ-plane and YZ-plane. While the cross polarizations (X-pol) at XZ-plane and YZ-plane are −42 dB and −43 dB, respectively. The merit of low cross polarization is obtained due to the purely directional field distribution of the TE_{101} mode, which has no field component at its orthogonal direction. The measured radiation patterns are in good agreement to the simulated ones. The small discrepancy is mainly due to the discontinuity on soldering between SMA and extended probe and the conductor loss of the cavity.

V. Conclusion

Low-sidelobe cavity-backed slot antenna arrays with simplified feeding structure for 5G-V2X communication are proposed in this paper. Low sidelobe is a good property for vehicular communication systems to improve the communication quality among vehicles or between vehicles and infrastructures. In this antenna, radiation slots are directly fed by the electric field of the cavity mode without utilizing any power dividers, which brings out a very simple antenna structure. Requirements of nonuniform amplitude and in-phase excitation for low-sidelobe antenna are easily obtained by adjusting the slots' sizes and positions. Three low-sidelobe antenna arrays with 1×4, 1×7, and 5×4 elements are presented and analyzed to show the flexible design feasibility. The proposed antenna shows the merits of simple antenna structure, high efficiency, high gain, low sidelobe, low cross-polarization. The measurement of the array with 5×4 elements has been conducted to validate the design concept. In fact, more slots can be accommodated on the top wall of the cavity and similar performance can be obtained. Besides, the full-metal structure introduces a high power-handling capacity.

References

[1] H. Wang, K. K. So, and X. Gao, "Bandwidth enhancement of a monopolar patch antenna with V-Shaped slot for car-to-car and WLAN communications," *IEEE Trans. Veh. Technol.*, vol. 65, no. 3, pp. 1130–1136, Mar. 2016.

[2] C.-X. Mao, S. Gao, and Y. Wang, "Dual-band full-duplex Tx/Rx antennas for vehicular communications," *IEEE Trans. Veh. Technol.*, vol. 67, no. 5, pp. 4059–4070, May 2018.

[3] X. Yang, P.-Y. Qin, Y. Liu, Y.-Z. Yin, and Y. J. Guo, "Analysis and design of a broadband multifeed tightly coupled patch array antenna," *IEEE Antennas Wireless Propag. Lett.*, vol. 17, no. 2, pp. 217–220, Feb. 2018.

[4] T. Mondal, S. Maity, R. Ghatak, and S. R. B. Chaudhuri, "Compact circularly polarized wide-beamwidth fern-fractal-shaped microstrip antenna for vehicular communication," *IEEE Trans. Veh. Technol.*, vol. 67, no. 6, pp. 5126–5134, Jun. 2018.

[5] L. Ge, S. Gao, Y. Li, W. Qin, and J. Wang, "A low-profile dual-band antenna with different polarization and radiation properties over two bands for vehicular communications," *IEEE Trans. Veh. Technol.*, vol. 68, no. 1, pp. 1004–1008, Jan. 2019.

[6] Z.-P. Zhong *et al.*, "A compact dual-band circularly polarized antenna with wide axial-ratio beamwidth for vehicle GPS satellite navigation application," *IEEE Trans. Veh. Technol.*, vol. 68, no. 9, pp. 8683–8692, Sep. 2019.

[7] G. Liu, Y.-M. Pan, and X.-Y. Zhang, "Compact filtering patch antenna arrays for marine communications," *IEEE Trans. Veh. Technol.*, vol. 69, no. 10, pp. 11408–11418, Oct. 2020.

[8] G.-L. Huang, S.-G. Zhou, T.-H. Chio, C.-Y.-D. Sim, and T.-S. Yeo, "Waveguide-stripline series-corporate hybrid feed technique for dual-polarized antenna array applications," *IEEE Trans. Compon., Packag. Manuf. Technol.*, vol. 7, no. 1, pp. 81–87, Jan. 2017.

[9] S.-G. Zhou, G.-L. Huang, and T.-H. Chio, "A lightweight, wideband, dual-circular-polarized waveguide cavity array designed with direct metal laser sintering considerations," *IEEE Trans. Antennas Propag.*, vol. 66, no. 2, pp. 675–682, Feb. 2018.

[10] B.-L. Zheng, S.-W. Wong, L. Zhu, and Y. He, "Broadband duplex-filtenna based on a low-profile metallic cavity packing," *IEEE Trans. Compon., Packag. Manuf. Technol.*, vol. 8, no. 8, pp. 1451–1457, Aug. 2018.

[11] X.-L. Lu, H. Zhang, S.-M. Gu, H. Liu, X.-C. Wang, and W.-Z. Lu, "A dual-polarized cross-slot antenna array on a parallel-plate waveguide with compact structure and high efficiency," *IEEE Antennas Wireless Propag. Lett.*, vol. 17, no. 1, pp. 8–11, Jan. 2018.

[12] S. Wang, L. Zhu, G. Zhang, J. Yang, J. Wang, and W. Wu, "Dual-band dual-CP all-metal antenna with large signal coverage and high isolation over two bands for vehicular communications," *IEEE Trans. Veh. Technol.*, vol. 69, no. 1, pp. 1131–1135, Jan. 2020.

[13] R.-S. Chen *et al.*, "High-efficiency and wideband dual-resonance full-metal cavity-backed slot antenna arrays," *IEEE Antennas Wireless Propag. Lett.*, vol. 18, no. 8, pp. 1360–1364, Aug. 2020.

[14] T. Varum, J. N. Matos, P. Pinho, and R. Abreu, "Nonuniform broadband circularly polarized antenna array for vehicular communications," *IEEE Trans. Veh. Technol.*, vol. 65, no. 9, pp. 7219–7226, Sep. 2016.

[15] F.-C. Chen, H.-T. Hu, R.-S. Li, Q.-X. Chu, and M. J. Lancaster, "Design of filtering microstrip antenna array with reduced sidelobe level," *IEEE Trans. Antennas Propag.*, vol. 65, no. 2, pp. 903–908, Feb. 2017.

[16] N. Boskovic, B. Jokanovic, and M. Radovanovic, "Printed frequency scanning antenna arrays with enhanced frequency sensitivity and sidelobe suppression," *IEEE Trans. Antennas Propag.*, vol. 65, no. 4, pp. 1757–1764, Apr. 2017.

[17] S. Ogurtsov and S. Koziel, "On alternative approaches to design of corporate feeds for low-sidelobe microstrip linear arrays," *IEEE Trans. Antennas Propag.*, vol. 66, no. 7, pp. 3781–3786, Jul. 2018.

[18] S.-J. Park, D.-H. Shin, and S.-O. Park, "Low side-lobe substrate integrated waveguide antenna array using broadband unequal feeding network for millimeter-wave handset device," *IEEE Trans. Antennas Propag.*, vol. 64, no. 3, pp. 923–932, Mar. 2016.

[19] Y.-J. Cheng, J. Wang, and X.-L. Liu, "94 GHz substrate integrated waveguide dual-circular-polarization shared-aperture parallel-plate long-slot array antenna with low sidelobe level," *IEEE Trans. Antennas Propag.*, vol. 65, no. 11, pp. 5855–5861, Nov. 2017.

[20] G.-L. Huang, S.-G. Zhou, T.-H. Chio, H.-T. Hui, and T.-S. Yeo, "A low profile and low sidelobe wideband slot antenna array feb by an amplitude-tapering waveguide feed-network," *IEEE Trans. Antennas Propag.*, vol. 63, no. 1, pp. 419–423, Jan. 2015.

[21] F.-C. Chen, J.-F. Chen, Q.-X. Chu, and M. J. Lancaster, "X-band waveguide filtering antenna array with nonuniform feed structure," *IEEE Trans. Microw. Theory Techn.*, vol. 65, no. 8, pp. 4843–4850, Dec. 2017.

[22] P. Kumar, A. Kedar, and A. K. Singh, "Design and development of low-cost low sidelobe level slotted waveguide antenna array in X-band," *IEEE Trans. Antennas Propag.*, vol. 63, no. 11, pp. 4723–4731, Nov. 2015.

[23] T. Mikulasek, J. Puskely, A. G. Yarovoy, J. Lacik, and H. Arthaber, "Transverse slot with control of amplitude and phase for travelling-wave SIW antenna arrays," *IET Microw., Antennas Propag.,* vol. 14, no. 15, pp. 1943–1946, Dec. 2020.

[24] R. Aslani, E. Saberinia, and M. Rasti,"Resource allocation for cellular V2X networks mode-3 with underlay approach in LTE-V standard," *IEEE Trans. Veh. Technol.*, vol. 69, no. 8, pp. 8601–8612, Aug. 2020.

[25] B. Feng, J. Chen, S. Yin, C.-Y.-D. Sim, and Z. Zhao,"A tri-polarized antenna with diverse radiation characteristics for 5G and V2X communications," *IEEE Trans. Veh. Technol.*, vol. 69, no. 9, pp. 10115–10126, Sep. 2020.

[26] R. Molina-Masegosa and J. Gozalvez, "LTE-V for sidelink 5G V2Xvehicular communications: A new 5G technology for short-range vehicle-to everything communications," *IEEE Veh. Technol. Mag.*, vol. 12, no. 4, pp. 30–39, Dec. 2017.

[27] C. L. Dolph, "A current distribution for broadside arrays which optimizes the relationship between beam width and side-lobe level," in *Proc. IRE Wave Electron.*, vol. 34, no. 6, pp. 335–348, Jun. 1946.

[28] C. A. Balanis, *Antenna Theory: Analysis and Design*, 3rd ed., Hoboken, NJ, USA: Wiley, 2005.

Rui-Sen Chen (Student Member, IEEE) was born in Fujian, China. He received the B.S. degree from the Hunan University of Science and Technology, Hunan, China, in 2012, and the master's degree in electromagnetic field and radio technology from the South China University of Technology, Guangzhou, China, in 2015. He is currently working toward theDoctor's degree with the College of Electronics and Information Engineering, Shenzhen University, Shenzhen, China. He was a Research Assistant with the Faculty of Science and Technology, University of Macau from January 2020 to December 2020. His current research interests include microwave filter, antenna, and cavity components.

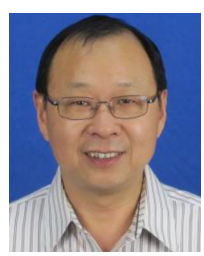

Lei Zhu (Fellow, IEEE) received the B.Eng. and M.Eng. degrees in radio engineering from the Nanjing Institute of Technology (now Southeast University), Nanjing, China, in 1985 and 1988, respectively, and the Ph.D. degree in electronic engineering from the University of Electro-Communications, Tokyo, Japan, in 1993. From 1993 to 1996, he was a Research Engineer with Matsushita-Kotobuki Electronics Industries Ltd., Tokyo, Japan. From 1996 to 2000, he was a Research Fellow with the École Polytechnique de Montréal, Montréal, QC, Canada. From 2000 to 2013, he was an Associate Professor with the School of Electrical and Electronic Engineering, Nanyang Technological University, Singapore. He joined the Faculty of Science and Technology, University of Macau, Macau, China, as a Full Professor in August 2013, and has been a Distinguished Professor since December 2016. From August 2014 to August 2017, he was the Head of the Department of Electrical and Computer Engineering, University of Macau. So far, he has authored or coauthored more than 630 papers in international journals and conference proceedings. His papers have been cited more than 10950 times with the H-index of 54 (source: Scopus). His research interests include microwave circuits, antennas, periodic structures, and computational electromagnetics. Dr. Zhu was the Associate Editor for the IEEE TRANSACTIONS ON MICROWAVE THEORY AND TECHNIQUES (2010–2013) and IEEE MICROWAVE AND WIRELESS COMPONENTS LETTERS (2006–2012). He was the General Chair of the 2008 IEEE MTT-S International Microwave Workshop Series on the Art of Miniaturizing RF and Microwave Passive Components, Chengdu, China, and a Technical Program Committee Co-Chair of the 2009 Asia–Pacific Microwave Conference, Singapore. He was the member of IEEE MTT-S Fellow Evaluation Committee (2013–2015), and as the member of IEEE AP-S Fellows Committee (2015–2017). He was the recipient of the 1997 Asia–Pacific Microwave Prize Award, the 1996 Silver Award of Excellent Invention from Matsushita-Kotobuki Electronics Industries Ltd., the 1993 Achievement Award in Science and Technology (first prize) from the National Education Committee of China, the 2020 FST Research Excellence Award from the University of Macau, and 2020 Macao Natural Science Award (second prize) from Science and Technology Development Fund (FDCT), Macau.

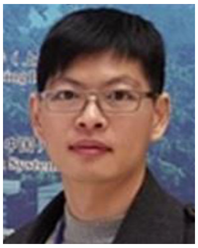

Sai-Wai Wong (Senior Member, IEEE) received the B.S. degree in electronic engineering from the Hong Kong University of Science and Technology, Hong Kong, in 2003, and the M.Sc. and Ph.D. degrees in communication engineering from Nanyang Technological University, Singapore, in 2006 and 2009, respectively. From July 2003 to July 2005, he was an Electronic Engineer to lead Electronic Engineering Department in China with two Hong Kong manufacturing companies. From May 2009 to October 2010, he was a Research Fellow with the ASTAR Institute for Infocomm Research, Singapore. Since 2010, he was an Associate Professor and later become a Full Professor with the School of Electronic and Information Engineering, South China University of Technology, Guangzhou, China. From July 2016 to September 2016, he was a Visiting Professor with the City University of Hong Kong. Since 2017, he has been a Full Professor with the College of Electronics and Information Engineering, Shenzhen University, Shenzhen, China. He has authored and coauthored more than 200 papers in international journals and conference proceedings. His current research interests include RF/microwave circuit and antenna design He was the recipient of the New Century Excellent Talents in University awarded by the Ministry of Education of China in 2013, and the Shenzhen Overseas High-Caliber Personnel Level C in 2018.

Xu-Zhou Yu received the B.E. degree from the School of Electronic and Information Engineering, Tianjin University, Tianjin, China, in 2019. He is currently working towards the master‘s degree with the College of Electronics and Information Engineering, Shenzhen University, Shenzhen, China. His current research interests include microwave cavity circuit design.

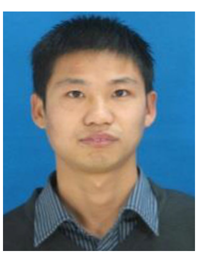

Yin Li (Member, IEEE) received the B. S. degree in applied physics from the China University of Petroleum, Dongying, China in 2009, the M. Eng. degree in electromagnetic field and microwave technology from the University of Electronic Science and Technology of China, Chengdu, China, in 2012, and the Ph.D. degree with the University of Macau, Macau, China. He is currently a Postdoctor Fellow with the School of Electronics and Information from Shen Zhen University, Shen Zhen, China. From 2013–2015, he was a Research Assistant with University of Hong Kong, Hong Kong, China. His current research interests include numerical modeling methods of passive microwave circuits, computational electromagnetics, microwave circuits, frequency selectivity surface, and filtering antenna.

Long Zhang (Member, IEEE) received the B.S. and M.S. degrees in electrical engineering from the Huazhong University of Science and Technology, Wuhan, China, in 2009 and 2012, respectively, and the Ph.D. degree in electronic engineering from the University of Kent, Canterbury, U.K., in 2017. He was a Research Fellow with Poly-Grames Research Center, Polytechnique Montreal, Canada. He is currently an Assistant Professor with the College of Electronics and Information Engineering, Shenzhen University, Shenzhen, China. His current research interests include circularly polarized antennas and arrays, mm-wave antennas and arrays, tightly coupled arrays, reflect arrays, and characteristics mode theory. Dr. Zhang was a Reviewer for several technique journals, including the IEEE TRANSACTIONS ON ANTENNAS AND PROPAGATION, the IEEE ANTENNAS AND WIRELESS PROPAGATION LETTERS, the *IET Microwaves, Antennas & Propagation, and the Electronic Letters.*

Yejun He (Senior Member, IEEE) received the Ph.D. degree in information and communication engineering from the Huazhong University of Science and Technology, Wuhan, China, in 2005. From 2005 to 2006, he was a Research Associate with the Department of Electronic and Information Engineering, Hong Kong Polytechnic University, Hong Kong. From 2006 to 2007, he was a Research Associate with the Department of Electronic Engineering, Faculty of Engineering, Chinese University of Hong Kong, Hong Kong. In 2012, he was a Visiting Professor with the Department of Electrical and Computer Engineering, University of Waterloo, Waterloo, ON, Canada. From 2013 to 2015, he was an Advanced Visiting Scholar (Visiting Professor) with the School of Electrical and Computer Engineering, Georgia Institute of Technology, Atlanta, GA, USA. Since 2011, he has been a Full Professor with the College of Electronics and Information Engineering, Shenzhen University, Shenzhen, China, where he is the Director of Guangdong Engineering Research Center of Base Station Antennas and Propagation, and the Director of the Shenzhen Key Laboratory of Antennas and Propagation, Shenzhen, China. He was awarded as Pengcheng Scholar Distinguished Professor, Shenzhen, China. He was also the recipient of Shenzhen Overseas High-Caliber Personnel Level B (“Peacock Plan Award” B) and Shenzhen High-Level Professional Tale (Local Leading Talent). He was the recipient of 2016 Shenzhen Science and Technology Progress Award and 2017 Guangdong Provincial Science and Technology Progress Award. He has authored or coauthored more than 200 research papers, books (chapters), and holds about 20 patents. His research interests include wireless communications, antennas, and radio frequency. Dr. He is an Associate Editor of the IEEE NETWORK, *International Journal of Communication Systems, China Communications*, and *Wireless Communications and Mobile Computing.* He was the General Chair of IEEE ComComAp 2019. He was a Reviewer for various journals such as the IEEE TRANSACTIONS ON VEHICULAR TECHNOLOGY, the IEEE TRANSACTIONS ON COMMUNICATIONS, IEEE TRANSACTIONS ON WIRELESS COMMUNICATIONS, THE IEEE TRANSACTIONS ON INDUSTRIAL ELECTRONICS, THE IEEE TRANSACTIONS ON ANTENNAS AND PROPAGATION, THE IEEE ANTENNAS AND WIRELESS PROPAGATION LETTERS, the IEEE WIRELESS COMMUNICATIONS, THE IEEE COMMUNICATIONS LETTERS, THE IEEE JOURNAL ON SELECTED AREAS IN COMMUNICATIONS, *International Journal of Communication Systems*, *Wireless Communications and Mobile Computing,* and *Wireless Personal Communications.* He has also served as a Technical Program Committee Member or a Session Chair for various conferences, including IEEE Global Telecommunications Conference (GLOBECOM), IEEE International Conference on Communications (ICC), IEEE Wireless Communication Networking Conference (WCNC), IEEE Vehicular Technology Conference (VTC), IEEE International Symposium on Antennas and Propagation (APS), European Conference on Antennas and Propagation (EuCAP), and Asia-Pacific Microwave Conference (APMC). He is the Principal Investigator for over 30 current or finished research projects including the NSFC of China, the Science and Technology Program of Guangdong Province as well as the Science and Technology Program of Shenzhen City. He is a Fellow of IET, and the Chair of IEEE Antennas and Propagation Society-Shenzhen Chapter.